Generation of milliCharged particles at the LHC

C. Campagnari, B. Marsh (UCSB), F. Golf (UNL)

July 9, 2019

1   Introduction

We discuss the MC generation of milliCharged particles (ζ) in pp collisions at the LHC in the central rapidity region. Except for Drell-Yan (DY), this is done in a few steps

1. Generate in various ways SM particles (A) that can decay as $A \to X\zeta^+\zeta^-$

2. Keep track of the cross-section for SM production of A.

3. Calculate the branching ratio for $A \to X\zeta^+\zeta^-$ for milliCharge $Q = 1$. For different charges, it is easy to scale the branching ratio as Q^2.

4. Generate the $A \to X\zeta^+\zeta^-$ decay with proper kinematics.

5. Save the "event" for further processing in a root file.

2   Special (simplest) case: Drell-Yan

The Drell-Yan process $pp \to \zeta^+\zeta^-$ is generated with the external model interface in MadGraph. Note: we cannot use SM $pp \to \ell^+\ell^-$ with a different lepton mass because the couplings of the Z to ζ's and leptons are different (in our model ζ's are weak isospin singlets[1][2]).
Status of this: this was done by Itay in MadGraph4, Golf is porting it to Madgraph5, but he has some bugs to fix.

3 List of non-DY processes

The main processes for $A \to e^+e^-X$ at the LHC are:

- $\pi^0 \to e^+e^-\gamma$ (BR=1.17%, Dalitz decay)

- $\eta \to e^+e^-\gamma$ (BR=0.7%, Dalitz decay)

- $\eta' \to e^+e^-\gamma$ (BR=5e-4, Dalitz decay)

- $\omega \to \pi^0 e^+e^-$ (BR=8e-4, Dalitz decay)

- $\eta' \to \omega e^+e^-$ (BR=2e-4, Dalitz decay)

- $\eta' \to \pi^+\pi^- e^+e^-$ (BR=2e-3, skip, see comment in Section 6)

- $V \to e^+e^-$ ($V = $ onia, ϕ, ρ, ω)

Note that if we are only interested in ζ masses above 100 MeV, Dalitz decays of π^0 and decays of η' into ω do not contribute. In all cases the BR for $A \to \zeta^+\zeta^-X$ can be obtained by rescaling $A \to e^+e^-X$ by a factor of Q^2 times an additional mass-dependent factor. In general this factor consists of a phase space piece $\sqrt{1 - (2m_\zeta/m_A)^2}$ plus an additional piece that arises from the matrix element.

Note: amongst these processes, the original [2] paper that proposed the milliqan experiment only included onia. Furthermore it is not clear that it included the $B \to \psi$ process, it is not clear that it included $\psi(2S)$, $\Upsilon(2S)$, and $\Upsilon(3S)$, and it imposed requirements $P_T > 6.5$ GeV (2 GeV) on J/ψ and $\Upsilon(1S)$, respectively. The Letter of Intent [3] also mentions $\Upsilon(2S)$ and $\Upsilon(3S)$, and it is possible that the latest NSF proposal included even more processes. In any case: here we make an attempt to include as many processes as possible and to remove P_T requirements.

4 Branching Ratios of non-DY processes (Q=1).

4.1 Dalitz BR

The partial width for $A \to e^+e^-\gamma$ can be written as[4, 5]:

$$\frac{d\Gamma}{dq^2} = \frac{2\alpha}{3\pi q^2} \ (1 + \frac{2m_e^2}{q^2}) \ \sqrt{1 - \frac{4m_e^2}{q^2}} \ (1 - \frac{q^2}{m_A^2})^3 \ |F(q^2)|^2 \ \Gamma(A \to \gamma\gamma) \quad (1)$$

where m_A is the mass of A, q^2 is the mass-squared of the e^+e^- pair, and $F(q^2)$ is a form factor. Note the $1/q^2$ factor that results in a highly non-uniform invariant mass distribution sharply peaked at low values. The form factor is such that $F(0) = 1$ and for pions is usually parametrized near $q^2 = 0$ as $F(q^2) = 1 + a\frac{q^2}{m_\pi^2}$ with $a \approx 0.03$. The form factor can also be estimated in the Vector Dominance Model (VDM) as

$$|F(q^2)|^2 = \frac{m_\rho^4 + m_\rho^2\Gamma_\rho^2}{(m_\rho^2 - q^2)^2 + m_\rho^2\Gamma_\rho^2} \tag{2}$$

where m_ρ and Γ_ρ are the mass and width of the ρ meson. The VDM model assumes that the decay proceeds through $\pi^0 \to \gamma V^*, V^* \to e^+e^-$ and $V = \rho$ or ω; equation 2 neglects the difference between ρ and ω.

In the case of $A \to e^+e^-X$, when X is not γ, the partial width can be written as

$$\frac{d\Gamma}{dq^2} = \frac{\alpha}{3\pi q^2} \left(1 + \frac{2m_e^2}{q^2}\right) \sqrt{1 - \frac{4m_e^2}{q^2}} \cdot$$
$$\left[\left(1 + \frac{q^2}{m_A^2 - m_X^2}\right)^2 - \frac{4m_A^2 q^2}{(m_A^2 - m_X^2)^2}\right]^{3/2} |F_{AX}(q^2)|^2 \ \Gamma(A \to X\gamma) \tag{3}$$

where m_X is the mass of X, and the transition form factor F_{AX} can also be approximated as in equation 2.

For milliCharged particles, Dalitz decays branching ratios can be obtained by integrating equation 1 or 3 from $q^2 = 4m_\zeta^2$ to the kinematical limit, substituting m_ζ for m_e, and rescaling by Q^2. Some numerical results for $Q = 1$ are given in Table 1. Note the sharp drop in branching ratios with mass. This is due to the $1/q^2$ behavior. The calculations with the electron and muon masses are in excellent agreement with the PDG.

4.2 Vector meson branching ratios

At lowest order the SM decay rate for $V \to \ell\ell$ is given by the Van Royen-Weisskopf formula[6, 7]:

$$\Gamma(V \to \ell\ell) = 4\pi\alpha^2 \frac{f_V^2}{m_V} Q_q^2 (1 - 4x_\ell^2)^{1/2}(1 + 2x_\ell^2) \tag{4}$$

3

m_ζ (MeV)	$\pi^0 \to \zeta\zeta\gamma$	$\eta \to \zeta\zeta\gamma$	$\eta' \to \zeta\zeta\gamma$	$\eta' \to \zeta\zeta\omega$	$\omega \to \zeta\zeta\pi^0$
0.511 $(=m_e)$	1.17 e-2	6.6 e-3	4.6 e-4	1.8 e-4	7.6 e-4
PDG for ee	(1.17 ± 0.04)e-2	(6.9 ± 0.4)e-4	(4.7 ± 0.3)e-4	(2.0 ± 0.4)e-4	(7.7 ± 0.6)e-4
10	2.8 e-3	2.9 e-3	2.5 e-4	5.7 e-5	3.7 e-4
30	3.5 e-4	1.6 e-3	1.8 e-4	1.7 e-5	2.3 e-4
50	1.2 e-5	1.0 e-3	1.4 e-4	4.3 e-6	1.6 e-4
60	2.7 e-7	8.2 e-4	1.3 e-4	1.7 e-6	1.4 e-4
90		4.3 e-4	1.0 e-4		9.2 e-5
105.7 $(=m_\mu)$		3.0 e-4	9.2 e-5		7.4 e-5
PDG for $\mu\mu$		(3.1 ± 0.4) e-4	(1.1 ± 0.3) e-4		(1.3 ± 0.2) e-4
150		8.9 e-5	6.8 e-5		3.7 e-5
200		1.2 e-5	4.8 e-5		1.5 e-5
250		1.0 e-7	3.2 e-5		3.6 e-6
400			5.6 e-7		

Table 1: Branching ratios for different Dalitz decay modes as a function of m_ζ for $Q = 1$ calculated based on equations 1, 2, and 3. When possible we compare with the values from the 2019 PDG.

where f_V is the vector decay constant, m_V is the vector mass, Q_q is the charge of the quark that makes up the meson, $x_\ell = m_\ell/m_V$, and m_ℓ is the lepton mass.

Thus the ratio of BR for $V \to \zeta\zeta$ to $V \to ee$ is given by

$$\frac{\Gamma(V \to \zeta\zeta)}{\Gamma(V \to ee)} = Q^2 \frac{(1 - 4x_\zeta^2)^{1/2}(1 + 2x_\zeta^2)}{(1 - 4x_\ell^2)^{1/2}(1 + 2x_\ell^2)} \tag{5}$$

where $x_\zeta = m_\zeta/m_V$, and m_ζ is the mass of ζ.

As a sanity check, we use equation 5 and BR($\psi(2S) \to ee$)=7.93e-3 to predict BR($\psi(2S) \to \tau\tau$) = 3.1e-3, in agreement with the PDG value of (3.1 $\pm$ 0.4)e-3.

5 Generation of SM particles decaying into $\zeta^+\zeta^-$
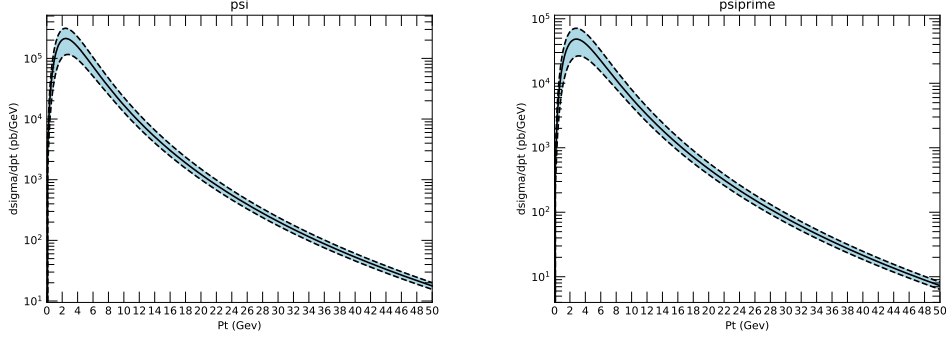
The key features of our approach are the following

Figure 1: Transverse momentum distributions of J/ψ (left) and ψ' from bottom quark decays. Note: this is from a single b, multiply by two to include $\bar{b}$. The units are pb/GeV and the distributions are integrated over $|\eta| < 1.0$.

- Use theory or published data, or some MC to generate P_T distributions for SM particles saved as histograms in ROOT files (Drell Yan is an exception, as discussed previously).

- Sample the ROOT histograms to generate SM particles of a given P_T.

- Pick azimuthal angles ϕ and pseudorapity η in a limited range, matched to the acceptance of milliqan. The η distribution is assumed to be flat, see comments in Section 6.

- Decay the SM particles into milliCharged particles.

- When possible, keep track of theoretical uncertainties.

- In general it is sufficient to generate SM particles at low and moderate P_T since that is where the cross-section is largest.

5.1 J/ψ and ψ' from b-decays

We use the tool available in
http://www.lpthe.jussieu.fr/ cacciari/fonll/fonllform.html
to generate histograms of P_T distributions (cross-sections) for charmonium from bottom decays, including theoretical uncertainties[9, 10]. See Figure 1
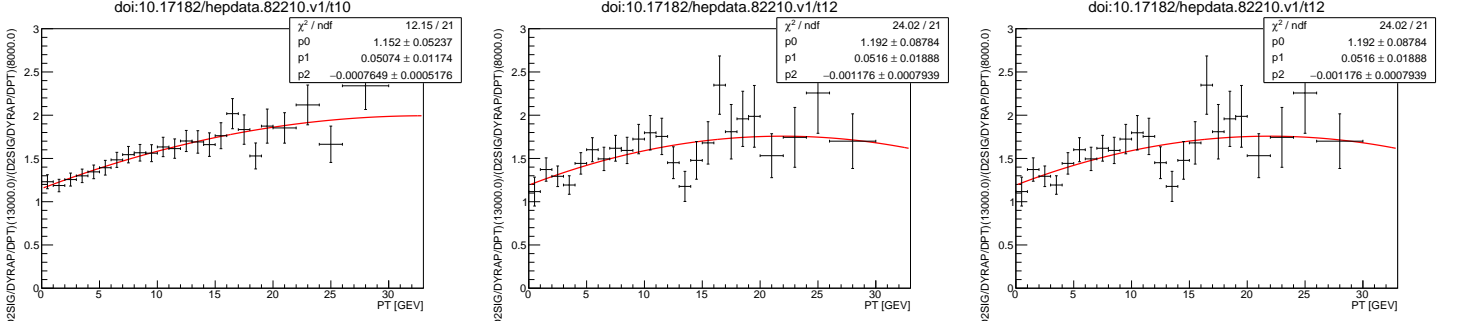
5

Figure 2: Ratio of 13 to 7 GeV Υ cross-section for $2.0 < y < 2.5$ from LHCb [17]. From left to right: 1S, 2S, 3S. The quadratic fits are ours.

5.2 Direct onia production

5.2.1 Direct bottonium

There have been many measurement of the P_T spectra od Υ in pp collisions at the LHC by CMS [11, 12, 13, 14], Atlas [15, 16], and LHCb [17, 18, 19, 20, 21]. The LHCb measurements are in the forward region. The only measurement at 13 TeV in the central region is from CMS [14]. Unfortunately, it is limited to $P_T > 20$ GeV.

Due to the lack of 13 TeV data, initially we planned to use theoretical predictions as a basis of the Υ event generation. We contacted the theorists [22] that provided the state-of-the art calculations used to confront the data in Reference [14]. We asked them to extend their predictions to lower P_T, unfortunately they claim that these are unreliable below 15 GeV.

As a result we decided to use 7 TeV data for $P_T < 20$ GeV and the CMS 13 TeV data at higher P_T. A key ingredient is the ratio of 13 and 7 GeV Υ production cross-sections. These have been measured for $P_T > 20$ GeV and $|\eta| < 1.2$ by CMS, see Figure 2 of Reference [14]. The ratios are about 1.7 at $P_T = 20$ GeV, irrespective of Υ state (1S, 2S, or 3S), and increase slowly to about 2 at $P_T = 40$ GeV. The ratios have also been measured by LHCb [17] all the way down to zero P_T for $2.0 < y < 2.5$, see Figure 2. The LHCb ratios in the 20-30 GeV region measured at slightly higher y are in agreement with the more central ratios measured by CMS.

Consequently, we rescale the **measured** 7 GeV **central** low P_T Υ spectra to 13 TeV using the curves of Figure 2; we combine these with the **measured** 13 TeV **central** high P_T spectra to obtain an inclusive 13 TeV spectra. The
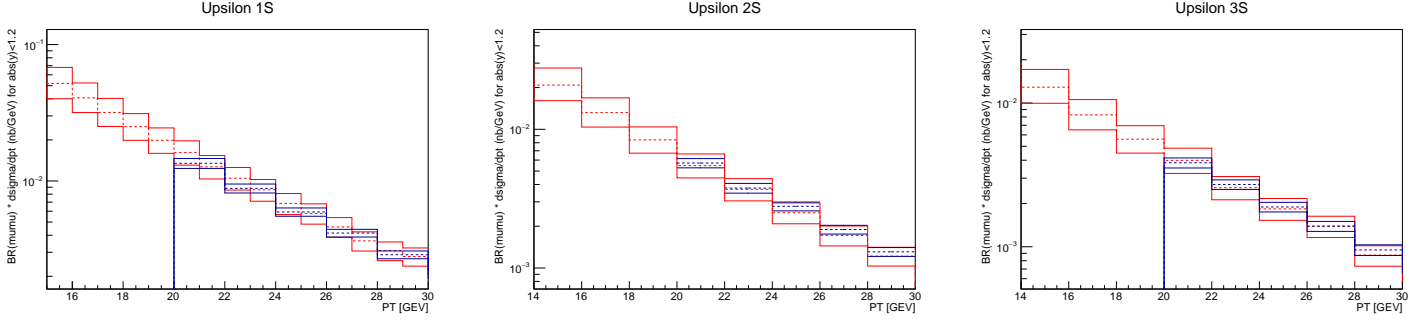
6

Figure 3: Comparison of the rescaled 7 GeV Atlas Υ spectra (red) with the 13 GeV CMS spectra (blue) in the neighborhood of 20 GeV, where the matching of the two spectra takes place. From left to right: 1S, 2S, 3S. The dashed lines represent the central values, the solid lines cover the uncertainty range. This is $\mathcal{B}(\Upsilon \to \mu\mu) \cdot \mathrm{d}\sigma/\mathrm{dP_T}$ in nb/GeV integrated over $|\eta| < 1.2$.
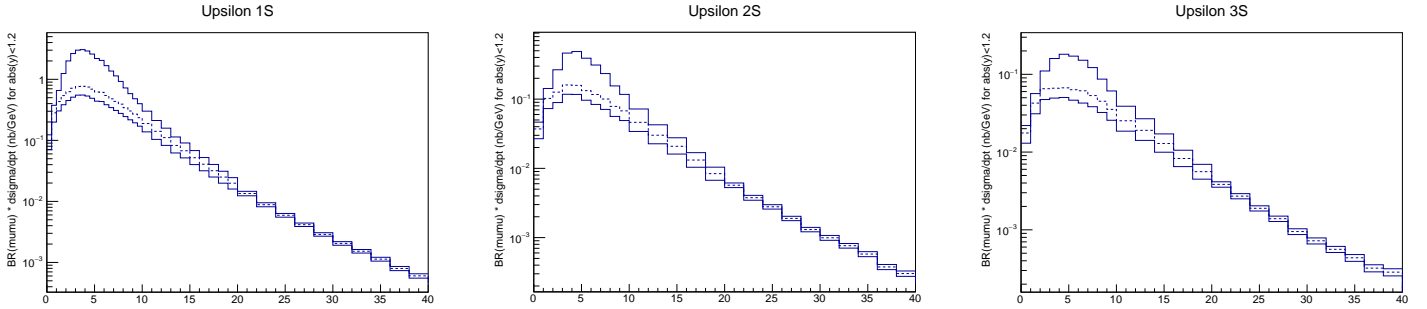

Figure 4: Combined Atlas 7 TeV, CMS 13 TeV Υ spectra. From left to right: 1S, 2S, 3S. The dashed line represent the central value, the solid lines cover the uncertainty range. This is $\mathcal{B}(\Upsilon \to \mu\mu) \cdot \mathrm{d}\sigma/\mathrm{dP_T}$ in nb/GeV integrated over $|\eta| < 1.2$.
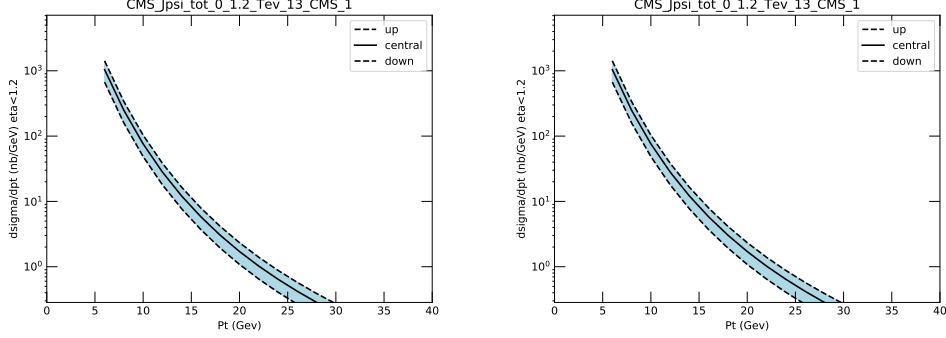
7

Figure 5: Transverse momentum distributions of J/ψ (left) and ψ' from direct production. The units are nb/GeV and the distributions are integrated over $|\eta| < 1.2$.

7 TeV data is from Atlas [16], since it happens to be in a more convenient format than the equivalent CMS data. On the other hand the 13 TeV spectra are from CMS [14], since there is no Atlas measurement at 13 TeV.

We demonstrate in Figure 3 that the matching of the Atlas and CMS cross-sections works well. The combined spectra to be used in the event generation are in Figure 4.

5.2.2 Direct charmonium

We take the charmonium spectra from theory [23, 24], see Figure 5. **NOTE: THESE ONLY GO DOWN TO 6 GEV BUT THE THEORISTS WILL PROVIDE CALCULATIONS TO LOWER PTs.**

5.3 π^0, η, η', ϕ, ρ, and ω

We generate these from Pythia. The measurement of the $\pi^\pm$ P_T spectrum from CMS[25] is in good agreement with Pythia 8 Minimum Bias at low momentum. This gives us some confidence in Pythia Min Bias, and consequently we use this MC for all mesons. We do not attempt to use QCD $2 \rightarrow 2$ at very low P_T since the process is infrared divergent.

Pythia `SoftQcd:nonDiffractive` includes all hard QCD processes[26] so in principle this is all that is needed. However, we run out of statistics at

8

high P_T. So at high P_T we stitch together the Min Bias distributions with distributions obtained from QCD $2 \rightarrow 2$ at moderate P_T.

Eventually we will generate Pythia events in "standalone" mode to be independent of CMS software. For now we use existing CMS Monte Carlos for Min Bias and for QCD. The CMS QCD samples are "P_T-binned", (15-30 GeV, 30-50 GeV, and 50-80 GeV). The Min Bias cross-section is taken to be 78.4 mb. Then the stitching procedure is the following:

- The QCD samples are first normalized to their LO cross-sections.

- Next, we estimate a "qcd-minbias scale factor" by integrating over some region where the ratio is roughly flat.

- The QCD samples are renormalized by this scale factor.

- The samples are stitched together by visually picking the P_T where the curves cross each other.

The resulting P_T curves are shown in Figure 6. It is not clear what kind of uncertainties we should assign. Eventually we'll have to come up with something (50%?).
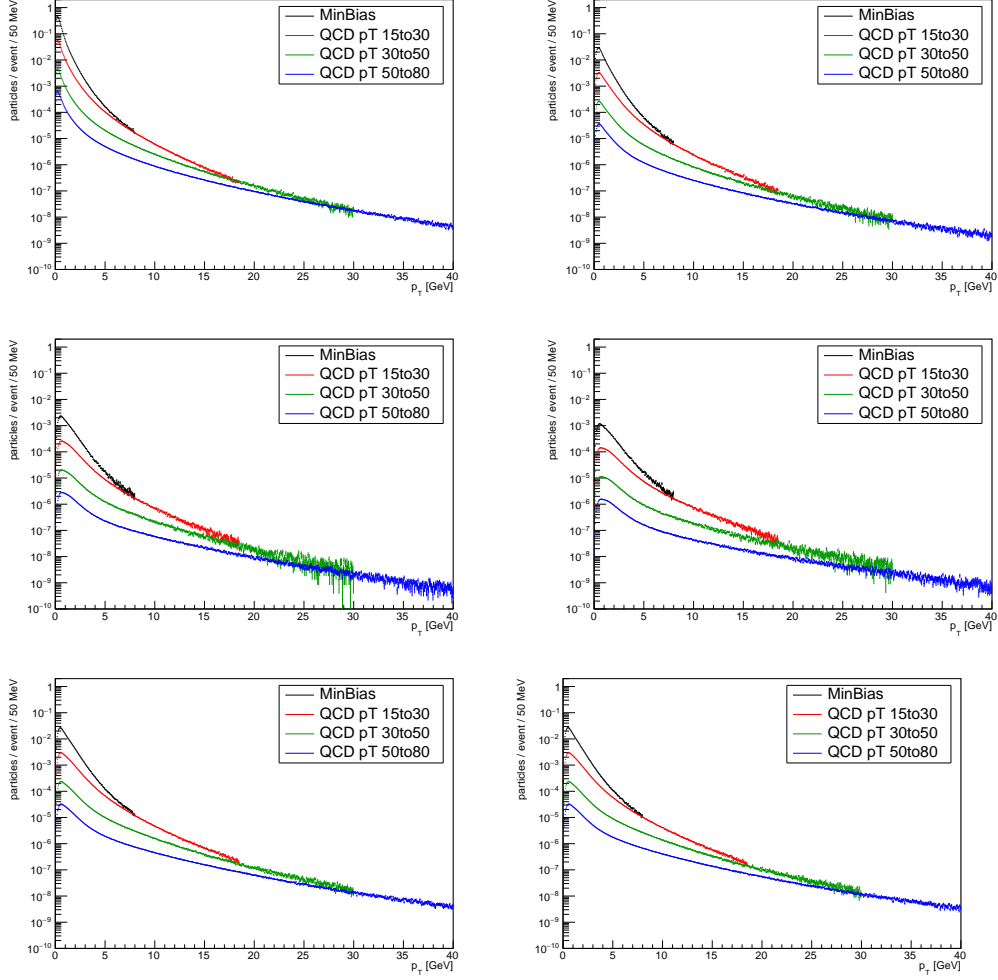
Figure 6: Transverse momentum distributions of π^0, η, η', ϕ, ρ, and ω, top left to bottom right, for $|\eta| < 1$.
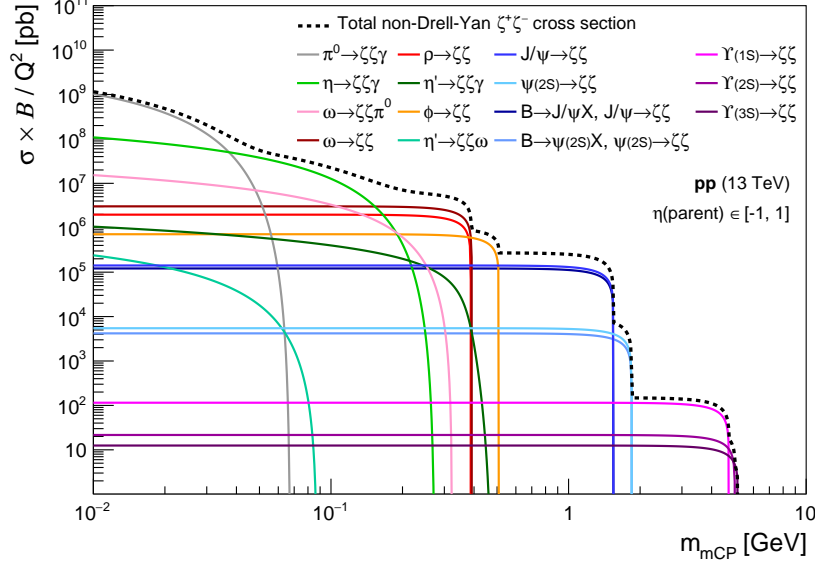
10

Figure 7: Cross-section times branching ratios for various decays into $\zeta^+\zeta^-$ pairs, excluding DY. Note: this is the cross section for producing the mother particle times the branching ratio for the mother particle to decay into $\zeta^+\zeta^-$. Multiply by two to get the $\zeta^\pm$ production cross section. Also: the mother particle must be in $|\eta| < 1$, but the daughter $\zeta^\pm$ could have $|\eta| > 1$. On the other hand some ζ's with $|\eta| < 1$ can arise from mothers of $|\eta| > 1$. The contribution from direct charmonium is not complete yet, see Section 5.2.2.

6   Putting cross sections and BR together

The total cross section for milliCharged particle production (excluding DY) is shown in Fig. 7. As mentioned in Section 3, we are skipping $\eta' \to \pi^+\pi^-\zeta^+\zeta^-$. Note that the other contributions from η' in the plot are neglogible. Since for $\zeta = e$ the branching ratio of the skipped process is four times higher than that of $\eta' \to e^+e^-\gamma$ (Dalitz decay), one worries that this process could actually be important. However, for reasonable ζ masses, say above 100 MeV, this process is suppressed by phase space with respect to Dalitz decay, e.g., from the PDG, $BR(\eta' \to \mu^+\mu^-\gamma) \approx$ 1e-4 while $BR(\eta' \to \pi^+\pi^-\mu^+\mu^-) <$ 3e-5. So we can safely ignore it.

 As mentioned in the caption of Figure 7 some of the ζ's in the central
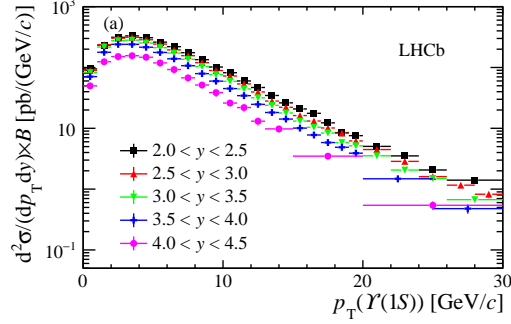
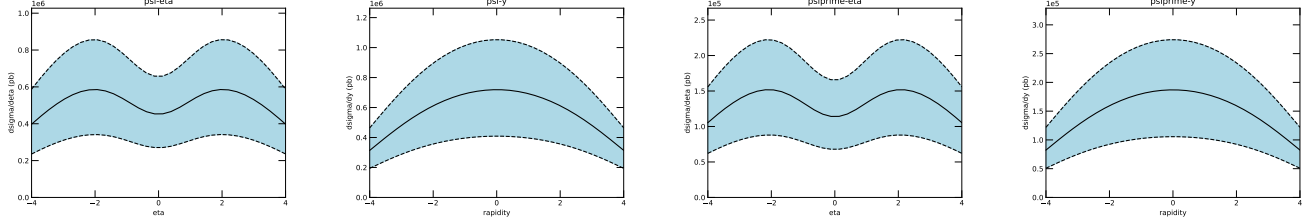Figure 8: $\Upsilon(1S)$ spectra in different rapidity ranges from LHCb [17].

Figure 9: Pseudorapidity and rapidity distributions from ψ (left) and $\psi(2S)$ (right) from b-decays[9, 10]. These are for $P_T < 10$ GeV, i.e., in the low boost regime. Note that in this P_T range the theoretical uncertainties are large.

region (i.e.: potentially within the acceptance of milliQan) could result from decays of mother particles at higher $|\eta|$, especially in the cases where the mother particles have low momentum and the boost in the decay is small. Particle production is nearly flat in rapidity, see Figures 8, 9 for some examples. The event generation will then assume a flat pseudorapidity distribution. At the analysis level one will be able to keep track of the contributions from high $|\eta|$ mothers, and assign a systematic if necessary.

7 Generation of the decays

We provide functions that take as input the lab frame 4-vector of either pseudoscalar (P) or vector (V) meson, and return the 4 vectors of the two ζ's from the decay. We assume that the V's are unpolarized.

7.1 Generation of pseudoscalar Dalitz decays

The implementation goes as follows (this also works for the Dalitz decay of the ω, whcih has J=1, as long as it is unpolarized):

- Rotate the 4-vector of P from the lab frame into frame S_1 such that P is traveling in the z-direction.

- Boost along z into frame S_2 where P is at rest.

- Pick a q^2 according to equation 1.

- Generate a decay $P \to X\gamma^*$ where γ^* is a particle of $m^2 = q^2$. The γ^* direction is random in ϕ and random in $\cos\theta$.

- Rotate the γ^* 4-vector into a frame S_3 such that the γ^* is traveling in the z-direction.

- Boost along z into frame S_4 where γ^* is at rest.

- Generate a decay $\gamma^* \to \zeta^+\zeta^-$ such that the angle ϕ of the ζ^+ is random and $\cos\theta$ is picked according to [8]

$$\frac{dN}{d\cos\theta} = 1 + \cos^2\theta + \frac{4m_\zeta^2}{q^2}\sin^2\theta \qquad (6)$$

- Set the 3-vector of the ζ^- to be back-to-back with the ζ^+.

- Boost the 4-vectors of the ζ's from S_4 to S_3.

- Rotate the 4-vectors of the ζ's from S_3 to S_2.

- Boost the 4-vectors of the ζ's from S_2 to S_1.

- Rotate the 4-vectors of the ζ's from S_1 to the lab frame.

13

7.2   Generation of vector decays

The procedure is the following:

- Rotate the 4-vector of V from the lab frame into frame S_1 such that V is traveling in the z-direction.

- Boost along z into frame S_2 where V is at rest.

- Generate a decay $V \to \zeta^+ \zeta^-$ such that both the angle ϕ and the $\cos \theta$ of the ζ^+ are random.

- Set the 3-vector of the ζ^- to be back-to-back with the ζ^+.

- Boost the 4-vectors of the ζ's from S_2 to S_1.

- Rotate the 4-vectors of the ζ's from S_1 to the lab frame.

References

[1] B. Holdom, Phys.Lett. B166, 196 (1986).

[2] A. Haas, C. S. Hill, E. Izaguirre and I. Yavin, Phys. Lett. B **746**, 117 (2015) doi:10.1016/j.physletb.2015.04.062 [arXiv:1410.6816 [hep-ph]].

[3] A. Ball *et al.*, arXiv:1607.04669 [physics.ins-det].

[4] L. G. Landsberg, Phys. Rep. 128, 301 (1985).

[5] See for example http://cds.cern.ch/record/683210/files/soft-96-032.pdf.

[6] Aloni, D., Efrati, A., Grossman, Y. et al. J. High Energ. Phys. (2017) 2017: 19.

[7] R. Van Royen and V. F. Weisskopf, Nuovo Cim. A 50, 617 (1967) Erratum: [Nuovo Cim. A 51, 583 (1967)].

[8] P. Adlarson et al., Phys. Rev. C 95, 025202 (2007).

[9] M. Cacciari, S. Frixione, N. Houdeau, M. L. Mangano, P. Nason and G. Ridolfi, JHEP **1210** (2012) 137 [arXiv:1205.6344 [hep-ph]].

[10] M. Cacciari, M. L. Mangano and P. Nason, arXiv:1507.06197 [hep-ph].

[11] V. Khachatryan *et al.* [CMS Collaboration], Phys. Rev. D **83**, 112004 (2011) doi:10.1103/PhysRevD.83.112004 [arXiv:1012.5545 [hep-ex]].

[12] S. Chatrchyan *et al.* [CMS Collaboration], Phys. Lett. B **727**, 101 (2013) doi:10.1016/j.physletb.2013.10.033 [arXiv:1303.5900 [hep-ex]].

[13] V. Khachatryan *et al.* [CMS Collaboration], Phys. Lett. B **749**, 14 (2015) doi:10.1016/j.physletb.2015.07.037 [arXiv:1501.07750 [hep-ex]].

[14] A. M. Sirunyan *et al.* [CMS Collaboration], Phys. Lett. B **780**, 251 (2018) doi:10.1016/j.physletb.2018.02.033 [arXiv:1710.11002 [hep-ex]].

[15] G. Aad *et al.* [ATLAS Collaboration], Phys. Lett. B **705** (2011) 9 doi:10.1016/j.physletb.2011.09.092 [arXiv:1106.5325 [hep-ex]].

[16] G. Aad *et al.* [ATLAS Collaboration], Phys. Rev. D **87**, no. 5, 052004 (2013) doi:10.1103/PhysRevD.87.052004 [arXiv:1211.7255 [hep-ex]].

[17] R. Aaij *et al.* [LHCb Collaboration], JHEP **1807** (2018) 134 Erratum: [JHEP **1905** (2019) 076] doi:10.1007/JHEP07(2018)134, 10.1007/JHEP05(2019)076 [arXiv:1804.09214 [hep-ex]].

[18] R. Aaij *et al.* [LHCb Collaboration], JHEP **1511** (2015) 103 doi:10.1007/JHEP11(2015)103 [arXiv:1509.02372 [hep-ex]].

[19] R. Aaij *et al.* [LHCb Collaboration], Eur. Phys. J. C **74** (2014) no.4, 2835 doi:10.1140/epjc/s10052-014-2835-1 [arXiv:1402.2539 [hep-ex]].

[20] R. Aaij *et al.* [LHCb Collaboration], JHEP **1306**, 064 (2013) doi:10.1007/JHEP06(2013)064 [arXiv:1304.6977 [hep-ex]].

[21] R. Aaij *et al.* [LHCb Collaboration], Eur. Phys. J. C **72**, 2025 (2012) doi:10.1140/epjc/s10052-012-2025-y [arXiv:1202.6579 [hep-ex]].

[22] H. Han, Y. Q. Ma, C. Meng, H. S. Shao, Y. J. Zhang and K. T. Chao, Phys. Rev. D **94**, no. 1, 014028 (2016) doi:10.1103/PhysRevD.94.014028 [arXiv:1410.8537 [hep-ph]].

[23] Y. Q. Ma, K. Wang and K. T. Chao, Phys. Rev. Lett. **106**, 042002 (2011) doi:10.1103/PhysRevLett.106.042002 [arXiv:1009.3655 [hep-ph]].

[24] Y. Q. Ma, K. Wang and K. T. Chao, Phys. Rev. D **84**, 114001 (2011) doi:10.1103/PhysRevD.84.114001 [arXiv:1012.1030 [hep-ph]].

[25] A. M. Sirunyan *et al.* [CMS Collaboration], Phys. Rev. D **96**, no. 11, 112003 (2017) doi:10.1103/PhysRevD.96.112003 [arXiv:1706.10194 [hep-ex]].

[26] http://home.thep.lu.se/t̃orbjorn/pythia81php/Welcome.php. Click on QCD on the left panel.